Carbohydrate Polymers 110 (2014) 224–230

Contents lists available at ScienceDirect

Carbohydrate Polymers

journal homepage: www.elsevier.com/locate/carbpol

Polyelectrolytic aqueous guar gum for adsorptive separation of soluble Pb(II) from contaminated water

Abhijit Pal, Tanbir Nasim, Arindam Giri, Abhijit Bandyopadhyay*

Department of Polymer Science and Technology, University of Calcutta, 92, A.P.C. Road, Kolkata 700009, India

ARTICLE INFO

Article history:
Received 2 December 2013
Received in revised form 7 March 2014
Accepted 20 March 2014
Available online 3 April 2014

Keywords:
Guar gum
Lead
Adsorption
Polyelectrolyte
Zeta potential

ABSTRACT

The article introduces the concept of homophase adsorption of soluble Pb(II) from contaminated water using aqueous guar gum (GG). The process appears to be extremely handy since it avoids hectic sample preparation and adsorbent recovery stages. The results show that, addition of only 1000 ppm GG removes 56.72% of the contaminated Pb(II) within 150 min at 303 K. The best working pH has been found to be at 4.5. At this point GG molecules show greatest balance between negative zeta potential and high molecular size. Mechanistically, the adsorption follows Langmuir model since on formation of a monolayer, the positive Pb(II) prevent subsequent adsorption through strong electrostatic repulsion. The adsorption kinetics follows pseudo second order model. Both kinetics and thermodynamics of the process complies with the conventional hetero facial adsorption models despite huge procedural differences.

1. Introduction

Water pollution is a major problem of the developing countries (Matlock, Howerton, & Atwood, 2001). One of the major reasons for water pollution is the direct contamination of heavy metal ions like Pb(II), Cd(II), Hg(II), Ni(II), Co(II), As(III) and Cr(VI) (Fu & Wang, 2011) in the surface water from various industrial effluents (Denizli, Sanli, Garipcan, Patir, & Alsancak, 2004; Han, Zhang, Zou, Shi, & Liu, 2005). The flora and fauna of the aquatic bodies absorb these metal ions. On feeding, the ions pass into the higher organisms and subsequently enter into the human food chain on consumption of these organisms (Chen & Wang, 2007). Beside, consuming these contaminated water bodies without proper pre-treatments also contaminates human body.

Pb(II) is the most common heavy metal ion found in the contaminated surface water. Paint industry, mining and plating industry, circuit board manufacturing units, electronic assembly plants, battery recycling plants, ferro-alloy manufacturing plants, ammunition, ceramic and glass industries, pulp, paper and paper board factories and several other chemical industries releases Pb(II) based effluents (Li & Bai, 2006). Industries under organized sector have proper effluent treatment facilities but medium and small scale industries, which are mainly under unorganized sector, hardly do any effluent treatments and release them to the surrounding water bodies. As per case studies, accumulation of Pb(II) in adult humans causes headaches, abdominal pain, poor appetite, constipation and anemia (Shiri, Ansari, Ranta, & Falah-Hassani, 2007). It also intervenes with the nervous system causing excessive irritation, aggression and sensitivity loss (Verity, 1990). As per medical reports, it has strong negative effects on children nervous systems and brains ensuing loss of development skills and IQ. In advanced stages (contamination above 0.05 ppm (Aydin, Yasar, Aydin, & Guzel, 2011)), it can also cause hearing loss and kidney damage.

Ion exchange (Aydin et al., 2011), evaporation (Leinen et al., 1996), flocculation (Fu & Wang, 2011), adsorption (Ghorai, Sinhamahpatra, Sarkar, Panda, & Pal, 2012; Gupta, Agarwal, Singh, & Pathania, 2013; Han et al., 2005; Pavasant et al., 2006), solvent extraction (Baba & Adekola, 2013), co-precipitation (Kagaya, Araki, Hirai, & Hasegawa, 2005), electrodialysis (Fu & Wang, 2011) and chelation therapy (Tandon, Singh, & Jain, 1994) are the prevalent unit operations for removal of Pb(II) from the contaminated water. However, the survey upholds adsorption as the most recommended process, not only for its high efficiency, but also for the energy economy for large scale operations (Denizli et al., 2004; Tran, Tran, & Nguyen, 2010). Both polymeric and non-polymeric adsorbents have been used at times in batch adsorption studies. Examples of some popular non-polymeric adsorbents include almond shell (Pehlivan, Altuna, Cetin, & Bhanger, 2009), grape stalks (Martinez et al., 2006), hazelnut shell (Pehlivan et al., 2009), waste maize bran (Singh, Talat, & Hasan, 2006) and clay (Chen & Wang, 2007). The main

* Corresponding author. Tel.: +91 033 235013976996/6387/8386x288.
E-mail addresses: abpoly@caluniv.ac.in, abhijitbandyopadhyay@yahoo.co.in (A. Bandyopadhyay).

http://dx.doi.org/10.1016/j.carbpol.2014.03.074
0144-8617/

difficulties with non-polymeric adsorbents are: (i) high sludge formation, (ii) requirement of subsequent unit process to remove the residual adsorbents and (iii) comparatively less efficient than the polymeric adsorbents. Alternatively, polymeric adsorbents, ideally composed of crosslinked biopolymer and semi-synthetic hydrogels, are more effective than the non-polymeric adsorbents. Finely chopped hydrogels are either added to the contaminated water or are packed in a column and the contaminated water is passed through at a specified rate. Chitosan (Zulkali, Ahmad, Norulakmal, & Sharifah, 2006), Chitosan/cellulose blends (Sun, Peng, Ji, Chen, & Li, 2009), Chitosan-g-PAA (Li & Bai, 2006), Poly(GMA-co-EGDMA)-en (Nastasovic et al., 2004) are examples of some common insoluble lead adsorbents. In each case, the sorption is swelling controlled and thus depends on the crosslink density and the interfacial area. Incidentally, both these parameters are physically very difficult to control. Moreover, recovery of the adsorbents (desorption) involves an extended unit process. Instead, we have introduced the concept of homophase adsorption in this article which is devoid of such limitations. Biopolymer solution in place of insoluble crosslinked gels have been used as adsorbents for soluble Pb(II) in the contaminated water. The advantages of this process are: (i) requirement of minimum polymer concentration, (ii) faster execution, (iii) no secondary contamination like leaching of the excess chemical crosslinkers from the hydrogels into the treated water and (iv) no recovery.

We have introduced guar gum solution (GG) as the new biosorbent in this article. GG is probably the commonest of all plant polysaccharides and is commercially available in the processed form. It has wide application as 'rheology modifier' in the foods and beverages (Butt, Shahzadi, Sharif, & Nasir, 2007). The microstructure of GG is shown in Fig. 1a. It has two building blocks composed of galactose and mannose connected through 1, 6 linkages. Previous examination shows the hydroxyl units are ionizable and imparts strong polyelectrolytic character (Nasim, Panda, & Bandyopadhyay, 2013). We have tried to explore this feature and its analogous effects for adsorption of soluble Pb(II) through electrostatic interaction. Extensive studies have been carried out through variation of all process parameters to maximize the adsorption efficiency. Process kinetics and thermodynamics are investigated to explain physical observations and further to compare with conventional interfacial adsorptions.

2. Materials and methods

2.1. Materials

Processed GG was a gifted sample received from Hindustan Gum and Chemicals Ltd., Haryana, India. Lead nitrate, Sodium acetate, Acetic acid, Hydrochloric acid, Sodium hydroxide and Xylenol orange indicator, all of standard laboratory grades, were procured from Merck, India. Ethylene diamine tetraacetic acid (EDTA) was purchased from Loba Chemie Pvt. Ltd., Mumbai, India. All the chemicals were used without further treatment and purification. Double distilled water was used throughout the experiments. Borosil glass materials were used for standard measurements and as apparatus.

2.2. Batch experiment for adsorption study

Adsorptions of Pb(II) over aqueous GG were studied in a batch process. About 0.399 g lead nitrate (MW: 331.24 g mol^{-1}) was dissolved in 250 ml double distilled water contained in a 250 ml volumetric flask to prepare a 1000 ppm (mg L^{-1}) stock model waste water. On the other hand, a 5000 ppm stock solution of GG was prepared by dissolving 0.5 g GG into 1000 ml double distilled water in a 1 L volumetric flask. 20 ml each of the original adsorbate and adsorbent solutions or their diluted forms as the case may be, were taken in a 100 ml conical flask and the pH of the mixture was adjusted to 1, 2, 3, 4, 4.5, 5, 5.5, 6, 6.5, 7, 8 and 9 by drop wise addition of 0.1 (N) HCl and NaOH solutions. The change in pH was monitored by a digital pH meter (APX, model: 175). Each flask was thermostated in an orbital shaker (Neolab, Kolkata, India) before the experiment. The experiments were conducted at various temperatures, shaking speeds and time to reach the adsorption equilibrium. On completion, the solution was centrifuged in a Remi Centrifuge, model: R8C for 15 min at 4000 rpm and then filtered using a Whatman® No. 40 filter paper. The clear filtrate was buffered (1:1) with sodium acetate- acetic acid at pH ≈5.0 and one drop of aqueous xylenol orange indicator was added. The solution was titrated using a standard EDTA solution until the color changes from intense red to yellow (Fig. 1b). The percentage adsorption of Pb(II) was calculated using Eq. (1):

$$\text{Adsorption}\,(\%) = \frac{C_0 - C_{eq}}{C_0} \times 100 \quad (1)$$

where C_0 is the initial and C_{eq} is the residual Pb(II) concentrations (mg L^{-1}). The adsorption values reported in each case are the numerical averages of three consecutive experiments.

The *Z*-average molecular sizes (mean hydrodynamic diameter) of the GG molecules under different experimental conditions were determined in a dynamic light scattering instrument (DLS, Zetasizer, model: Nano-ZS90) procured from Malvern Instruments Ltd., United Kingdom. The zeta potentials of both Pb(II) and GG molecules were determined in the same instrument.

3. Results and discussion

3.1. Effect of pH

Fig. 2 shows the effect of pH on adsorption efficiency of aqueous GG. The agitation speed and contact time are arbitrarily set at 120 rpm and 150 min. The concentrations of GG and Pb(II) are maintained at 1000 and 100 ppm. The profile shows presence of four interesting stages. Initially between pH 1.0 and 2.0, the adsorption efficiency remains zero. However, beyond 2.0, there is a steep rise in efficiency which is maintained up to 4.5. Between pH 4.5 and 6.0 is the zone of "minimum change" wherein the efficiency marginally decreases even on changing the pH by 1.5 units. Finally, beyond 6.0, on further increase in pH raises the efficiency to 100%. The *Z*-average molecular sizes and zeta potentials of the adsorbent molecules at the experimental pH are plotted in the same figure. Between pH 1.0 and 2.0, the GG molecules assume positive potentials due to protonation of its hydroxyl units (+1.68 and +0.11 mV). However, in spite of having higher molecular sizes (1615 and 1758 d nm) due to strong intermolecular repulsion, the molecules finally show zero adsorption efficiency as the positive surface charges of the GG molecules strongly repel the positive Pb(II). Beyond 2.0, the extent of adsorption increases mainly due to conversion of positive zeta potentials of GG into negative values since the hydroxyl units are difficult to protonate under low acidic conditions. In this region, the average sizes of the molecules also decrease due to intermolecular repulsion with increase in negative charge density (Nasim & Bandyopadhyay, 2012). The adsorption trend shows that a maximum of 56.72% of the contaminated Pb(II) are removed at pH 4.5. At this point, the zeta potential is −1.12 mV and the average size is 1371 d nm. Between 4.5 and 6.0, the adsorption efficiency decreases by 5.38% which is possibly due to faster decrease in adsorbent sizes compared to its zeta potentials (Fig. 2). In previous two stages, even though the zeta potentials of the GG molecules dominate adsorption efficiency but in the third stage, the molecular size plays the leading role. Beyond 6.3, extremely low solubility of lead hydroxide causes all Pb(II) to precipitate

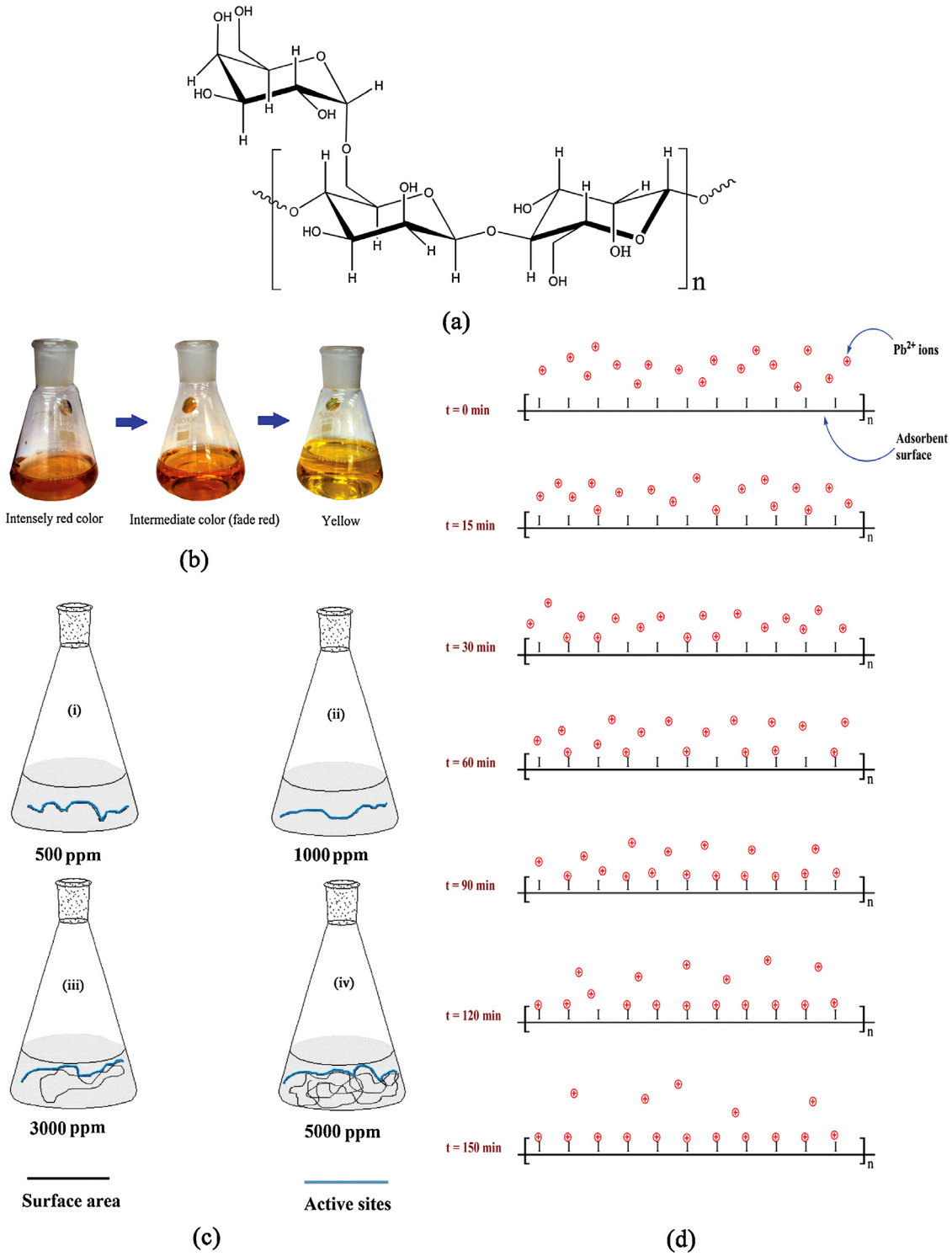

Fig. 1. (a) Microstructure of GG molecules, (b) change of color during titrimetric determination of Pb(II) concentrations, (c) a schematic showing non-proportionality between *Z*-average molecular sizes of aqueous GG and its active sites and (d) a schematic showing time dependent adsorption of Pb(II) over active sites of aqueous GG.

(Namasivayam & Ranganathan, 1995) which eventually shows a 100% removal of Pb(II) from the contaminated water.

3.2. *Effect of adsorbent concentration*

Fig. 3a shows the change in adsorption efficiency on changing GG concentrations. All studies have been carried out at pH 4.5 since it has produced the maximum removal efficiency. However, the agitation speed and contact time are kept constant at 120 rpm and 150 min. Starting from 500 ppm, the GG concentration is gradually increased up to 5000 ppm. At 500 ppm, 33.43% of the contaminated Pb(II) are adsorbed which drastically increases to 56.72% at 1000 ppm but then slightly decreases and finally produces 48.87% adsorption efficiency at 5000 ppm. Since the pH remains constant, zeta potentials of the GG molecules do not vary and has no role to play instead, the molecular sizes becomes prime important in controlling the adsorption efficiency. The concentration dependent molecular sizes of GG are plotted in Fig. 3a. It shows a steady rise

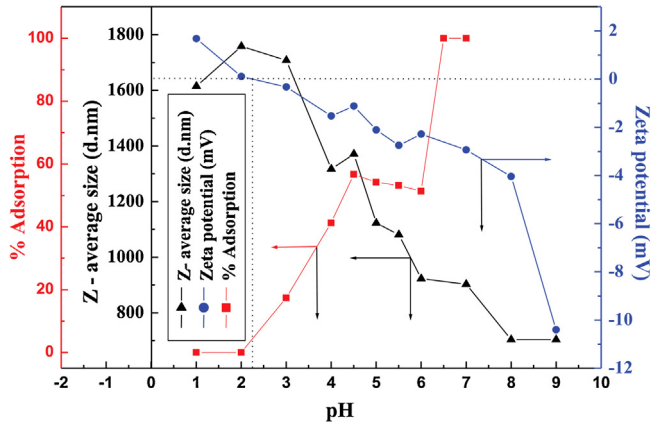

Fig. 2. A four axes plot (three *Y* and one *X*) showing the effect of pH on adsorption efficiency, zeta potential and *Z*-average molecular sizes of aqueous GG.

but without any positive effect on adsorption efficiency. We presume this rise in molecular size as the intermolecular "aggregation effect" of many GG molecules aided by the hydrogen bonded interaction between active hydroxyl units. These aggregates grow in size on increasing the GG concentration. Fig. 1c pictorially demonstrates this effect using arbitrary molecules. The aggregation effect eventually reduces available adsorbent area and thus a slight drop in adsorption efficiency has been recorded beyond 1000 ppm GG concentration.

3.3. Effect of contact time and agitation speed

Fig. 3b shows the effect of changing contact time and agitation speed on adsorption efficiency. The experiments are carried out at pH 4.5 using 1000 ppm GG concentration. At 60 rpm agitation speed, the adsorption efficiency gradually increases with increasing contact time as greater contact time allows more Pb(II) to interact with the GG molecules. The adsorption efficiency achieves maxima close to 150 min. At this point, the adsorbent molecules become saturated, possibly due to occupation of all available sites. Fig. 1d shows a demonstration of the "time effect" on adsorption. It is interesting to note that, even with a minimum contact time of 20 min aqueous GG is capable of adsorbing nearly 30% of the contaminated Pb(II). However, using the best contact time, the adsorption efficiency is found to increase with increasing agitation speed. This trend is maintained up to 120 rpm. Beyond that, the efficiency marginally decreases (around 3%). At higher

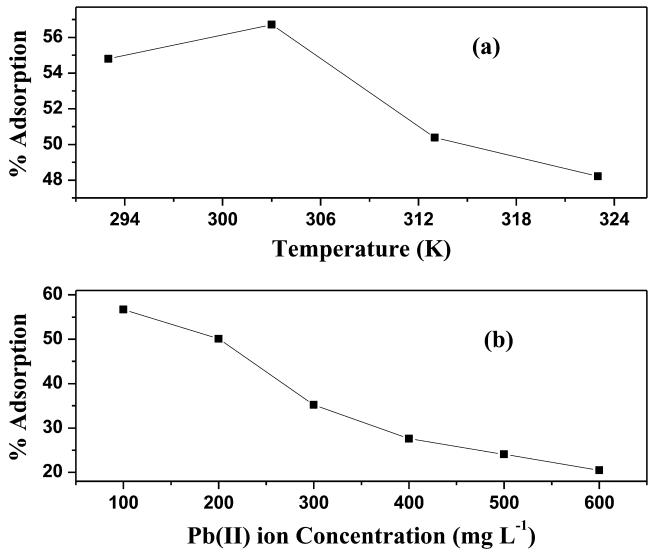

Fig. 4. Adsorption efficiency of aqueous GG at various (a) temperature and (b) concentrations of Pb(II).

agitation speed (rotation), the heavier components like GG molecules and Pb(II) move downwards from the central position of the flask. Due to such movements, greater contact between GG and Pb(II) becomes statistically feasible which aids the adsorption efficiency. But at extremely high speed, the adsorption efficiency decreases due to high Brownian movements of the components. However, it is important to note that even with zero agitation speed by only providing 150 min contact time the GG molecules are capable of adsorbing 26.94% of the contaminated Pb(II).

3.4. Effect of temperature and concentration of Pb(II)

Using the best possible conditions, effect of temperature and concentration of Pb(II) on adsorption efficiency has been investigated. The results are plotted in Fig. 4. At 293 K, the adsorption efficiency is 54.79%. It maximizes to 56.72% at 303 K but thereafter decreases on further raising the temperature. Rise in temperature causes greater solubilization of GG molecules. This leads to more unfolding of the molecules and generation of more active sites. Availability of more active sites at 303 K compared to 293 K increases adsorption efficiency. However, rise in temperature simultaneously increases Brownian movements of the

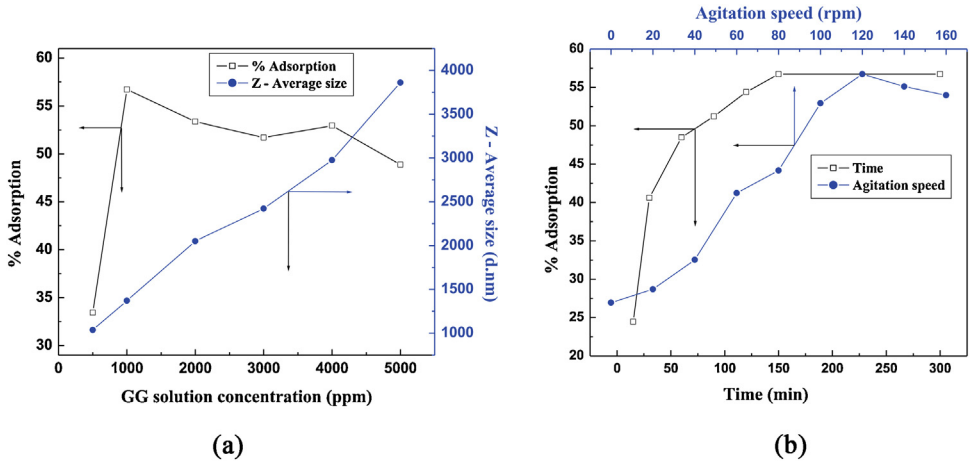

Fig. 3. (a) A three axes (two *Y* and one *X*) plot showing the correlations between adsorption efficiency, solution concentration and *Z*-average molecular sizes of GG molecules and (b) a three axes plot (two *X* and one *Y*) showing the effect of contact time and agitation speed on adsorption efficiency of aqueous GG.

components. On dominance, the later leads to more "desorption" of the ions from the active sites of the GG molecules. Thus beyond 303 K, due to dominance of the Brownian movements, a drop in adsorption efficiency has been noted. However, a steady drop in adsorption efficiency is noted on increasing Pb(II) concentrations as well. With all other parameters remaining constant, the number of active sites on the adsorbent molecules is supposed to be fixed. The results indicate that, under similar condition, the sites get saturated in presence of 100 ppm Pb(II). On doubling the ion concentration, the adsorption efficiency decreases to 50.09% which means nearly 100 ppm out of 200 ppm virtually remains unadsorbed. Similarly, on quadrupling the concentration (400 ppm), the efficiency drops to 27.6% i.e. nearly 300 ppm of Pb(II) remains unaffected.

3.5. Construction of adsorption isotherm: Langmuir vs. Freundlich models

Adsorption isotherm delineates adsorption mechanism. Under best processing condition, the adsorption efficiency obtained at 303 K against different Pb(II) concentrations are used to construct the two premier isotherm models.

Presumption of the Langmuir model is the formulation of a monolayer of the adsorbate (Pb(II)) over the adsorbent (GG). The mathematical representation of the model is:

$$q_{eq} = \frac{Q_m b C_{eq}}{1 + bC_{eq}} \quad (2)$$

Here C_{eq} is the equilibrium concentration of the adsorbate (Pb(II)) in mg L^{-1} and q_{eq} is the equilibrium concentration of the adsorbate in mg g^{-1}. The q_{eq} is calculated using the formula stated in Eq. (3):

$$q_{eq} = (C_0 - C_{eq}) \times \frac{v}{W} \quad (3)$$

Q_m in Eq. (2) is the adsorption capacity of the adsorbent (GG) and b is the Langmuir constant in L mg^{-1} which is equivalent to the heat of adsorption. The linear form of the model can be represented as:

$$\frac{C_{eq}}{q_{eq}} = \frac{1}{Q_m b} + \frac{C_{eq}}{Q_m} \quad (4)$$

A plot of (C_{eq}/q_{eq}) vs. C_{eq} should produce a straight line in order to follow this model. Fig. 5a shows the plot. It also shows the Q_m and b values calculated from the slope and the intercept of the best fit straight line. These along with Q_m and b values calculated at two other temperatures (293 and 313 K) along with necessary error analysis data are reported in Table 1. The Regression coefficient, R^2, shows extremely high fitment accuracy with the experimental data in every case as they approach very close to unity.

Often a dimensionless number called separation factor, R_L is calculated to confirm the fitment accuracy of the Langmuir model (Ghorai et al., 2012). R_L is calculated using the Eq. (5):

$$R_L = \frac{1}{1 + bC_0} \quad (5)$$

where C_0 is the initial concentration of Pb(II) expressed in mg L^{-1}. Supplementary Table 1 lists the R_L values for each Pb(II) concentration. All values lie between 0 and 1 which confirms high fitment accuracy of the adsorption data with the Langmuir model.

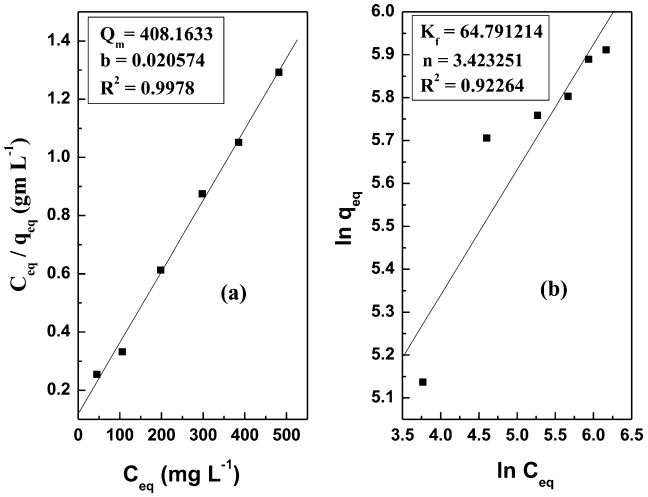

Fig. 5. Adsorption isotherms of Pb(II) at 303 K (a) Langmuir model and (b) Freundlich model.

Supplementary material related to this article can be found, in the online version, at http://dx.doi.org/10.1016/j.carbpol.2014.03.074.

Freundlich adsorption model is related to multilayer adsorption where multiple layers of adsorbates are formed over the adsorbent surfaces. The mathematical form of the model is an empirical one which is expressed as in Eq. (6):

$$q_{eq} = K_f C_{eq}^{1/n} \quad (6)$$

Here, K_f and n are Freundlich constants corresponding to the non- ideal adsorption mechanism. The linear form of the model is expressed as:

$$\ln q_{eq} = \ln K_f + \frac{1}{n} \ln C_{eq} \quad (7)$$

A plot of $\ln q_{eq}$ against $\ln C_{eq}$ should produce a straight line in order to follow this model. Fig. 5b shows the plot. K_f and n values are calculated from the intercept and the slope of the best fit straight line and are denoted in the figure. Table 1 reports these values at 293, 303 and 313 K. The Regression coefficient, R^2, show poor fitment accuracy with the experimental data than the Langmuir model. It is physically agreeable since formation of a monolayer of Pb(II) will always repel the subsequent adsorption of the another layer of Pb(II).

However, we have compared the Q_m data obtained from the Langmuir model for aqueous GG with some of the highly cited polymeric and non-polymeric adsorbents used for removing Pb(II). This is listed in Supplementary Table 2 (Atia, Donia, & Yousif, 2008, Chang, Law, & Chang, 1997, Deng, Su, Su, Wang, & Zhu, 2007, Liu, Chang, Guo, & Meng, 2006, Meesri, Praphairaksit, & Imyim, 2007, Naseem & Tahir, 2001, Ramirez, Burillo, Barrera-Diaz, Roa, & Bilyeu, 2011, Singh, Tiwari, Sharma, & Sanghi, 2007, Wan, Kan, Rogel, & Dalida, 2010 and Zhang et al., 2008). It shows that, except the work done with a biocomposite by Ghorai et al. (2012), the adsorption capability of aqueous GG is found to be far ahead of the rest of the adsorbents studied for the past 16 years.

Table 1
Adsorption isotherm data at three different temperatures with necessary error analysis data and standard deviation.

Temperature (K)	Langmuir model					Freundlich model				
	Q_m (mg g^{-1})	Error	b (L mg^{-1})	R^2	SD	K_f (mg g^{-1})	n	Error	R^2	SD
293	408.1633	5.0	0.015669	0.9960	0.03151	60.1433	3.389831	0.05219	0.93289	0.11873
303	408.1633	0.1	0.020574	0.9978	0.03036	64.79121	3.423251	0.06125	0.92264	0.12372
313	408.1633	3.0	0.011601	0.9942	0.03078	41.02945	2.805757	0.05773	0.96741	0.11326

Table 2
Adsorption kinetics and thermodynamics data.

(a) Kinetic data for various non linear models.

Kinetics model	Equation	Plot	Regression coefficient (R^2)	Standard deviation (SD)
Pseudo first order	$\log(q_{eq} - q_t) = \log q_{eq} - \frac{k_1 t}{2.303}$	$\log(q_{eq} - q_t)$ vs. t	0.98724	0.0803
Pseudo second order	$\frac{t}{q_t} = \frac{1}{k_2 q_{eq}^2} + \frac{t}{q_{eq}}$	(t/q_t) vs. t	0.99913	0.02446
Second order	$\frac{1}{q_{eq} - q_t} = \frac{1}{q_{eq}} + k_3 t$	$(1/(q_{eq} - q_t))$ vs. t)	0.93548	0.02156
Intraparticle diffusion	$q_t = k_4 t^{1/2} + I$	q_t vs. $t^{1/2}$	0.8374	0.02087

(b) Thermodynamic data at 293, 303 and 313 K.

Temperature (K)	ΔG° (kJ mol^{-1})	ΔH° (kJ mol^{-1})	ΔS° (kJ mol^{-1} K^{-1})
293	−20.955		
303	−22.236	16.5783	0.1281
313	−21.447	−45.2337	−0.0759

Supplementary material related to this article can be found, in the online version, at http://dx.doi.org/10.1016/j.carbpol.2014.03.074.

3.6. Investigations on adsorption kinetics and thermodynamics

Referring to the kinetic data shown in Fig. 3b, it is clear that the non-linear trend does not match with either zero order or first order kinetic models. We tried to fit these data in non-linear models like pseudo first order, pseudo second order, second order and intraparticle diffusion models. The linear forms of these models are listed in Table 2(a). For each model, the necessary parameters are also mentioned which should be plotted to check the linear fit accuracy of the data. On performing such actions and comparing each Regression coefficient, R^2, it is seen that the adsorption data is best fitted into pseudo second order kinetic model. In this model, the rate limiting step is assumed as the surface adsorption phase aided by chemisorption. This is followed in the present study since under medium acidity, the negative zeta potentials of GG favors effective adsorption of the positive Pb(II) through strong chemical interactions. This is also the best fit kinetic model for interfacial adsorption of various metal ions other than Pb(II). Thus, the present study is found to be kinetically complied with the standard interfacial adsorption studies (Fig. 6).

The equilibrium free energies at 293, 303 and 313 K are calculated using Gibbs free energy isotherm equation (Eq. (8)).

$$\Delta G^\circ = -RT \ln b \tag{8}$$

From the free energy values enthalpy and entropy were also calculated using Gibbs free energy equation (Eq. (9)) which is constructed from Van't Hoff equation (Eq. (10)).

$$\Delta G^\circ = \Delta H^\circ - T\Delta S^\circ \tag{9}$$

$$\ln b = \frac{-\Delta H^\circ}{RT} + \frac{\Delta S^\circ}{R} \tag{10}$$

Table 2(b) represents the values of ΔG°, ΔH° and ΔS°. Correlating these with the adsorption efficiencies reported in Fig. 4a shows that, due to less negative values at both 293 and 313 K, the

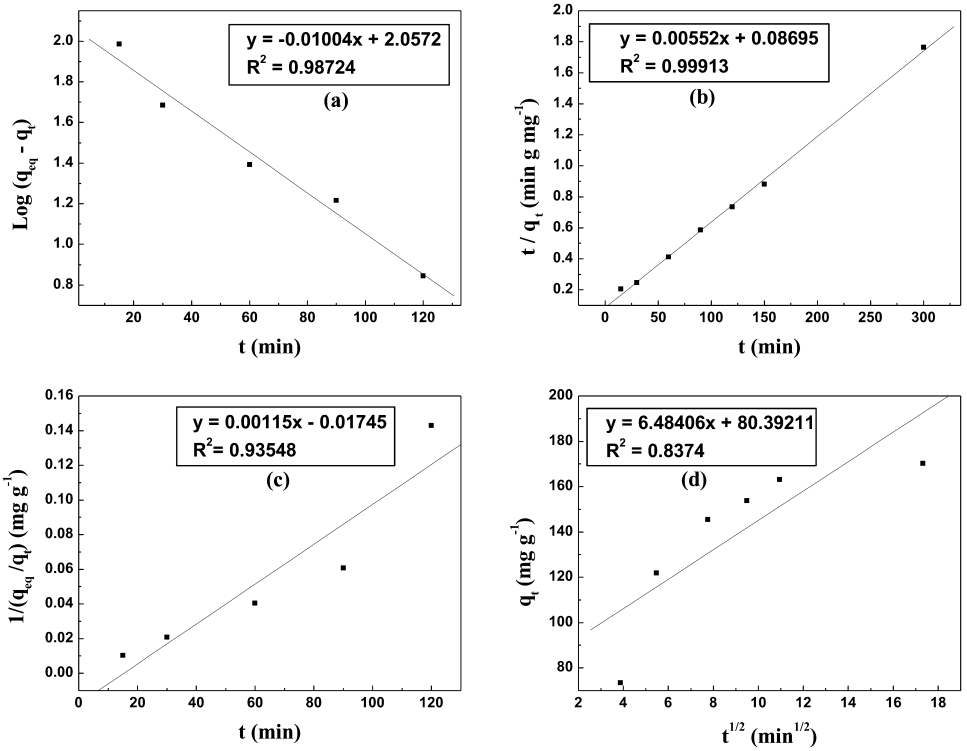

Fig. 6. Fitment of the kinetic data for adsorption of Pb(II) over GG molecules in (a) pseudo first order, (b) pseudo second order, (c) second order and (d) intraparticle diffusion models.

efficiencies are low compared to 303 K wherein, due to most negative free energy value the efficiency is maximum. Various other adsorbents used for adsorption of Pb(II) also have shown similar range of free energies at these temperatures. Alike interfacial adsorption kinetics, the process is thus thermodynamically complied as well. Positive value of enthalpy change (ΔH°) eventually confirmed the endothermic nature of the sorption process. Positive value of ΔS° confirms good affinity of Pb(II) toward GG molecules.

4. Conclusions

GG solution is thus found to be highly efficient in adsorbing soluble Pb(II) from contaminated water. The process is handy since the complicated sample preparation steps in solid adsorption process could be avoided. Calculations revealed that the process is kinetically and thermodynamically complied with the conventional adsorption studies. At the best working condition aqueous GG removes 56.72% of the contaminated Pb(II) through monolayer formation from an initial Pb(II) concentration of 100 ppm. However, the process is yet to reach the WHO recommended Pb(II) limit (0.05 ppm) in the safe drinking water. Thus further investigation is on the cards to increase the efficiency of the process.

Acknowledgement

The authors wish to acknowledge TEQIP (Technical Education Quality Improvement Programme) Phase II, University of Calcutta (TEQIP-II/ACA/12/PST/001) for providing financial support to undertake this research work.

References

Atia, A. A., Donia, A. M., & Yousif, A. M. (2008). Removal of some hazardous heavy metals from aqueous solution using magnetic chelating resin with iminodiacetate functionality. *Separation and Purification Technology*, *61*, 348–357.

Aydin, F., Yasar, F., Aydin, I., & Guzel, F. (2011). Determination of lead separated selectively with ion exchange method from solution onto BCW in Sirnak, East Anatolia of Turkey. *Microchemical Journal*, *98*, 246–253.

Baba, A. A., & Adekola, F. A. (2013). Solvent extraction of Pb(II) and Zn(II) from a Nigerian galena ore leach liquor by tributylphosphate and bis(2,4,4-trimethylpentyl)phosphinic acid. *Journal of King Saud University – Science*, *25*, 297–305.

Butt, M. S., Shahzadi, N., Sharif, M. K., & Nasir, M. (2007). Guar gum: A miracle therapy for hypercholesterolemia, hyperglycemia and obesity. *Critical Reviews in Food Science and Nutrition*, *47*(4), 389–396.

Chang, J.-S., Law, R., & Chang, C.-C. (1997). Biosorption of lead, copper and cadmium by biomass of Pseudomonas aeruginosa PU21. *Water Research*, *31*(7), 1651–1658.

Chen, H., & Wang, A. (2007). Kinetic and isothermal studies of lead ion adsorption onto palygorskite clay. *Journal of Colloid and Interface Science*, *307*, 309–316.

Deng, L., Su, Y., Su, H., Wang, X., & Zhu, X. (2007). Sorption and desorption of lead (II) from wastewater by green algae Cladophora fascicularis. *Journal of Hazardous Materials*, *143*, 220–225.

Denizli, A., Sanli, N., Garipcan, B., Patir, S., & Alsancak, G. (2004). Methacryloylamidoglutamic acid incorporated porous poly(methyl methacrylate) beads for heavy-metal removal. *Industrial & Engineering Chemistry Research*, *43*, 6095–6101.

Fu, F., & Wang, Q. (2011). Removal of heavy metal ions from wastewaters: A review. *Journal of Environmental Management*, *92*, 407–418.

Ghorai, S., Sinhamahpatra, A., Sarkar, A., Panda, A. B., & Pal, S. (2012). Novel biodegradable nanocomposite based on XG-g-PAM/SiO2: Application of an efficient adsorbent for Pb^{2+} ions from aqueous solution. *Bioresource Technology*, *119*, 181–190.

Gupta, V. K., Agarwal, S., Singh, P., & Pathania, D. (2013). Acrylic acid grafted cellulosic Luffa cylindrical fiber for the removal of dye and metal ions. *Carbohydrate Polymers*, *98*, 1214–1221.

Han, R., Zhang, J., Zou, W., Shi, J., & Liu, H. (2005). Equilibrium biosorption isotherm for lead ion on chaff. *Journal of Hazardous Materials*, *125*, 266–271.

Kagaya, S., Araki, Y., Hirai, N., & Hasegawa, K. (2005). Coprecipitation with yttrium phosphate as a separation technique for iron(III), lead, and bismuth from cobalt, nickel, and copper matrices. *Talanta*, *67*, 90–97.

Leinen, D., Caballero, A., Fernandez, A., Espinos, J. P., Justo, A., Gonzalez-Elipe, A. R., et al. (1996). Structural characterization of $PbTiO_3$ thin films prepared by ion beam induced CVD and evaporation of lead. *Thin Solid Films*, *272*, 99–106.

Li, N., & Bai, R. (2006). Highly enhanced adsorption of lead ions on chitosan granules functionalized with poly(acrylic acid). *Industrial & Engineering Chemistry Research*, *45*(23), 7897–7904.

Liu, Y., Chang, X., Guo, Y., & Meng, S. (2006). Biosorption and preconcentration of lead and cadmium on waste Chinese herb Pang Da Hai. *Journal of Hazardous Materials B*, (135), 389–394.

Martinez, M., Miralles, N., Hidalgo, S., Fiol, N., Villaescusa, I., & Poch, J. (2006). Removal of lead(II) and cadmium(II) from aqueous solutions using grape stalk waste. *Journal of Hazardous Materials*, *133*, 203–211.

Matlock, M. M., Howerton, B. S., & Atwood, D. A. (2001). Irreversible precipitation of mercury and lead. *Journal of Hazardous Materials*, *84*, 73–82.

Meesri, S., Praphairaksit, N., & Imyim, A. (2007). Extraction and preconcentration of toxic metal ions from aqueous solution using benzothiazole-based chelating resins. *Microchemical Journal*, *87*, 47–55.

Namasivayam, C., & Ranganathan, K. (1995). Removal of lead(II) by adsorption onto waste iron(III)/chromium(III) hydroxide from aqueous solution and radiator manufacturing industry wastewater. *Industrial & Engineering Chemistry Research*, *34*, 869–873.

Naseem, R., & Tahir, S. S. (2001). Removal of Pb(II) from aqueous/acidic solutions by using bentonite as an adsorbent. *Water Research*, *35*(16), 3982–3986.

Nasim, T., & Bandyopadhyay, A. (2012). Introducing different poly (vinyl alcohol)s as new flocculant for kaolinated waste water. *Separation and Purification Technology*, *88*, 87–94.

Nasim, T., Panda, A. B., & Bandyopadhyay, A. (2013). Guar gum and guar gum-oligomeric poly(vinyl alcohol) blends as novel flocculants for kaolinated waste water. *International Journal of Biological Macromolecules*, *58*, 140–147.

Nastasovic, A., Jovanovic, S., Dordevic, D., Onjia, A., Jakovljevic, D., & Novakovic, T. (2004). Metal sorption on macroporous poly(GMA-co-EGDMA) modified with ethylene diamine. *Reactive & Functional Polymers*, *58*, 139–147.

Pavasant, P., Apiratikul, R., Sungkhum, V., Suthiparinyanont, P., Wattanachira, S., & Marhaba, T. F. (2006). Biosorption of Cu^{2+}, Cd^{2+}, Pb^{2+}, and Zn^{2+} using dried marine green macroalga Caulerpa lentillifera. *Bioresource Technology*, *97*, 2321–2329.

Pehlivan, E., Altuna, T., Cetin, S., & Bhanger, M. I. (2009). Lead sorption by waste biomass of hazelnut and almond shell. *Journal of Hazardous Materials*, *167*, 1203–1208.

Ramirez, E., Burillo, S. G., Barrera-Diaz, C., Roa, G., & Bilyeu, B. (2011). Use of pH-sensitive polymer hydrogels in lead removal from aqueous solution. *Journal of Hazardous Materials*, *192*(2), 432–439.

Shiri, R., Ansari, M., Ranta, M., & Falah-Hassani, K. (2007). Lead poisoning and recurrent abdominal pain. *Industrial Health*, *45*, 494–496.

Singh, K. K., Talat, M., & Hasan, S. H. (2006). Removal of lead from aqueous solutions by agricultural waste maize bran. *Bioresource Technology*, *97*, 2124–2130.

Singh, V., Tiwari, S., Sharma, A. K., & Sanghi, R. (2007). Removal of lead from aqueous solutions using *Cassia grandis* seed gum-graft-poly(methylmethacrylate). *Journal of Colloid and Interface Science*, *316*, 224–232.

Sun, X., Peng, B., Ji, Y., Chen, J., & Li, D. (2009). Chitosan(Chitin)/cellulose composite biosorbents prepared using ionic liquid for heavy metal ions adsorption. *Separations*, *55*(8), 2062–2069.

Tandon, S. K., Singh, S., & Jain, V. K. (1994). Efficacy of combined chelation in lead intoxication. *Chemical Research in Toxicology*, *7*, 585–589.

Tran, H. V., Tran, L. D., & Nguyen, T. N. (2010). Preparation of chitosan/magnetite composite beads and their application for removal of Pb(II) and Ni(II) from aqueous solution. *Materials Science and Engineering: C*, *30*(2), 304–310.

Verity, M. A. (1990). Comparative observations on inorganic and organic lead neurotoxicity. *Environmental Health Perspectives*, *89*, 43–48.

Wan, M.-W., Kan, C.-C., Rogel, B. D., & Dalida, M. L. P. (2010). Adsorption of copper (II) and lead (II) ions from aqueous solution on chitosan-coated sand. *Carbohydrate Polymers*, *80*(3), 891–899.

Zhang, G., Qu, R., Sun, C., Ji, C., Chen, H., Wang, C., et al. (2008). Adsorption for Metal Ions of Chitosan Coated Cotton Fiber. *Journal of Applied Polymer Science*, *110*(4), 2321–2327.

Zulkali, M. M. D., Ahmad, A. L., Norulakmal, N. H., & Sharifah, N. S. (2006). Comparative studies of Oryza sativa L. husk and chitosan as lead adsorbent. *Journal of Chemical Technology and Biotechnology*, *81*(7), 1324–1327.